PHYSICAL REVIEW A VOLUME 22, NUMBER 3 SEPTEMBER 1980

Experimental determination of the relativistic fine-structure splitting in pionic Ti and Fe atoms

K.-C. Wang,* F. Boehm, E. Bovet, A. A. Hahn, H. E. Henrikson, J. P. Miller,† R. J. Powers, P. Vogel, and J.-L. Vuilleumier
California Institute of Technology, Pasadena, California 91125

A. R. Kunselman
University of Wyoming, Laramie, Wyoming 82071
(Received 3 April 1980)

Using a high-resolution crystal spectrometer we have measured the relativistic angular-momentum splittings of the $5g$-$4f$ and $5f$-$4d$ transitions in pionic Ti and Fe atoms. The observed fine-structure splittings of 85.3 ± 3.0 eV in π^- Ti and 158.5 ± 7.8 eV in π^- Fe agree with the calculated splittings of 88.5 and 167.6 eV, respectively, arising from the Klein-Gordon equation and from small corrections due to vacuum polarization, strong interaction, and electron screening.

INTRODUCTION

The breaking of the accidental degeneracy in bound states of spin-$\frac{1}{2}$ particles, such as electrons or negative muons, in the Coulomb field of a nucleus is an extensively studied and well-established phenomenon. The Dirac equation successfully explains the observed features. There has been little experimental work, however, on the degeneracy breaking in the bound states of a spin-zero particle in a Coulomb field. The resulting fine-structure splitting is expected to obey a relativistic equation for bosons, such as the Klein-Gordon equation. The present work is concerned with this degeneracy breaking in a pionic atom. An experimental study is presented of the energy splitting of states possessing the same principal quantum number but different orbital quantum numbers.

In recent years researchers in pionic atoms have begun to focus on this question. Carter *et al.*[1] have examined the fine-structure splitting for the $n = 6$-5 and 7-6 pionic transitions in heavy nuclei of Au, Tl, and Pb. More recently, the present Caltech group,[2] using a high-resolution crystal diffraction technique has measured the fine-structure doublet associated with the transitions $5g$-$4f$ and $5f$-$4d$ in pionic Ti. A similar experiment on Ti was also reported by Delker *et al.*[3]

Subsequent to the preliminary presentation of the Caltech results by Wang *et al.*,[2] measurements on the fine-structure splitting in pionic Fe have been undertaken. The purpose of this paper is to present a full account of the π-Ti and π-Fe experiments followed by a discussion of the results in the framework of a computation of the pionic-atom bound states based on the Klein–Gordon equation. The observed fine-structure splitting can be compared to the calculated splitting as obtained from an expansion in $(\alpha Z/n)^2$ of the Klein-Gordon energy eigenvalue. In choosing relatively high principal and angular-momentum quantum numbers, one ensures that the effects of finite nuclear size and strong interaction are minimized. The atoms of Ti and Fe were selected for practical reasons including the suitability of the transition energy for the crystal spectrometer technique.

The first section gives a description of the experimental arrangement and results. A presentation of the calculation is given in the second section. Auxiliary information bearing on the comparison between the Klein-Gordon and relativistic Schrödinger equations is contained in the Appendix.

EXPERIMENTAL METHOD AND RESULTS

The experiment was carried out at the East leg of the stopped muon channel at Los Alamos Meson Physics Facility (LAMPF). The layout of the experiment is shown in Fig. 1. Negative pions of momentum 140 MeV/c were selected by the channel magnets and focused on the target. The experimental area consisted of three parts: (1) The target area with the pion-beam degrader and the x-ray production targets; (2) the crystal cave which contained the curved quartz crystal, the sine screw, and a Ge(Li) monitor detector; and (3) the slit cave which contained the curved receiving slit and an array of four intrinsic Ge detectors. The control and data signals were connected to an on-line computer. Each part of the experimental setup is briefly sketched below. Detailed descriptions of other aspects of the work can be found in Ref. 4.

Target area. For the Ti (Fe) measurements the beam spot size was 10 cm wide and 6 cm high (6 cm wide and 1.4 cm high). The thickness of the polyethylene degrader was 12 cm and was adjusted

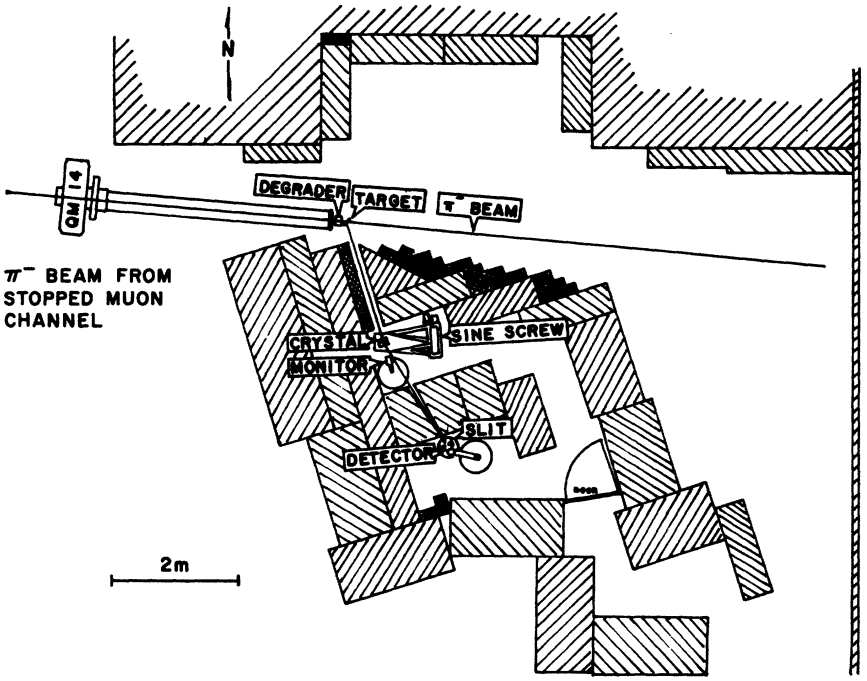

FIG. 1. Layout of the experiment showing last beam-line magnet (QM14) of East leg of muon channel at LAMPF, spectrometer cave, and experimental setup.

to maximize the 5-4 pionic x-ray yield in a monitor detector. Two metallic Ti targets of 1.3 g/cm^2 thickness (areas 10×10 and 14×10 cm^2) and a metallic Fe target 1.5 g/cm^2 thick were used. The π^- stopping rate was about 10^7 π^-/sec. Approximately 10^6 pionic 5-4 x rays were emitted per second from the Ti or Fe target. These rates include x-ray self-absorption in the target.

Caltech-LAMPF bent-crystal spectrometer. The bent-crystal spectrometer used for this experiment has been described in detail in Ref. 5. The spectrometer consists of two units, the crystal unit and the slit-detector unit. They were mounted in two independent, well-shielded concrete caves, as illustrated in Fig. 1. The curved crystal at 2.3 m distance from the target consisted of a 11.5 ×9-cm^2 quartz slab (310 reflecting planes), 0.13 cm thick, with an aperture of 5×7 cm^2. A Hartmann test showed that the bending radius R was 201.1 cm and the width of the aberration pattern at the focal position was 0.12 mm, which corresponds to a resolution of 18.5 eV at 40.5 keV and 36.2 eV at 56.6 keV.

The pionic x rays were diffracted in first order and focused into a resolving slit which had a width of 0.15 mm for the Ti measurement and 0.08 mm for the Fe measurement. For the extended source and extended slit geometry[5] used with the spectrometer, the locus of the focal points is given by the intersection of a cone and a cylinder of radius $R\cos^2\theta$. The slit thus was curved with a radius of 197.5 cm and had its azimuthal direction adjustable to match the x-ray wavelength. The detector array behind the slit consisted of four high-purity Ge detectors,[6] each of which was 4-cm high, 0.5-cm wide, and 0.5-cm thick, and had an energy resolution of 1-keV FWHM (full width at half-maximum) at 40 keV.

The resolution of the bent-crystal spectrometer had contributions from the aberrations of the focal spot of the crystal, the slit width, the size of the source, and the crystal mosaic spread.[7] The compound resolution was found to be 32-eV FWHM for the π^--Ti 5-4 transitions and 55-eV FWHM for the π^--Fe 5-4 transitions.

Monitor detector. A monitor Ge(Li) detector viewing the Ti or Fe target was set behind the crystal out of the way of the diffracted pionic x rays (see Fig. 1). It had an energy resolution of 0.6-keV FWHM at 40 keV. The counts under the pionic 4-3 peak seen by the monitor were used to normalize the counting rate of the Ge detectors.

Background. Due to the low efficiency (~10^{-8}) of the bent-crystal spectrometer and the high background of neutrons and gamma rays at LAMPF, the background problem was critical for the feasibility of the precision experiment under discussion. The separation of the spectrometer into two parts, with a 1.2-m thick concrete wall between them, helped to reduce the background consider-

TABLE I. Comparison of the wavelengths λ, the Bragg angles θ, and the natural linewidths Γ, of the calibration electronic *x* rays.

		Wavelength λ(mÅ)[a]	Bragg angle θ(°)	Natural linewidth Γ(mÅ)[b]
Eu	$K\alpha_1$	298.452(2)	7.26	0.179
	$K\alpha_2$	303.124(2)	7.38	0.187
Sm	$K\alpha_1$	309.046(2)	7.52	0.182
	$K\alpha_2$	313.704(2)	7.64	0.189
Tm	$K\beta_1$	215.56(2)	5.24	0.153
	$K\beta_3$	213.36(2)	5.26	0.154
Er	$K\beta_1$	222.66(2)	5.41	0.156
	$K\beta_3$	223.41(2)	5.43	0.157

[a] The wavelengths are taken from Ref. 9 and are given in mÅ. λ(mÅ) = 1.000 020 5(56) λ(mÅ*).[12]

[b] Data taken from Ref. 11. Errors of the natural linewidths are estimated to be 3%.

ably. A 10-cm lead shield surrounding the detector array and the good energy resolution of the Ge detectors further helped to reduce the background which was about 0.2 counts/min in a window encompassing the 5-4 x-ray peaks.

Data taking and results. The angular position of the crystal was determined with a precision sine screw,[8] the angular increments being proportional to the wavelength increments δλ. The $K\alpha_{1,2}$ x rays of Eu and Sm were used as calibration lines for the Ti measurement, while $K\beta_{1,3}$ x rays of Tm and Er served to calibrate the pionic Fe line. The wavelengths[9] of these calibration x rays were very close to those of the pionic lines under investigation, as can be seen in Tables I and II. These x rays were produced by fluorescent excitation of the respective oxide targets using the 59.54-keV gamma line of a strong ^{241}Am source. The observed $K\alpha_1$ and $K\alpha_2$ x-ray profiles were analyzed by comparing them with the convolution of Gaussian and Lorentzian functions over a linear background.[10] The natural linewidths[11] are given in Table I. The observed $K\beta_{1,3}$ profiles were fitted to the sum of two Gaussian functions over a linear background.

Aberrational errors originating from the finite size of the source were taken into account with a "response matrix" established by a detailed study of the correlation between the position of the reflected x rays from the present crystal and the corresponding locus of convergence.

The pionic 5*g*-4*f* and 5*f*-4*d* peaks were continuously scanned in rapid succession. In the Ti case, a scan encompassed 18 to 22 wavelength positions with a step size of 0.10 mÅ (13.2 eV). One scan lasted about three hours and 62 scans were taken. In the Fe case, a scan consisted of 31 positions with a step size of 0.05 mÅ (13.0 eV) and 32 scans were taken. For each spectrometer position the energy spectra of the Ge detectors and the monitor detector were recorded. To optimize the statistical accuracy of the splitting, the measurement periods for the weak peak (5*f*-4*d*) were chosen to be four times longer than those for the strong peak (5*g*-4*f*). For the Ti measurement, we divided the total scans into three groups. In group I, which contained 50% of the total data, a Ti target of a size 10×10 cm^2 was used. In groups II and III, which contained 10% and 40% of the total data, respectively, a 14×10 cm^2 target was used. Between groups II and III, the target position was lowered by 0.25 cm. The data of the three groups were analyzed separately. In the Fe measurement, only one target size and one target position were utilized.

The pionic 4-3 peak recorded concurrently in the monitor Ge(Li) served to normalize the crystal spectrometer data. The normalized wavelength spectra were obtained by summing the pulse height spectra of the four Ge counters in the energy intervals of 40.5 ± 1.0 keV, and 56.6 ± 1.0 keV, for Ti and Fe, respectively. The wavelength spectra are depicted in Figs. 2 and 3.

The final spectra were then fitted to the sum of two Gaussian functions with identical widths above a linear background. The widths of the Gaussian functions were determined from the calibration x-ray lines using the natural widths of Table I, as well as from the ^{241}Am 59.54-keV gamma line. In the least-squares fits, the two amplitudes and two centroids of the Gaussian functions and the background parameters were allowed to vary. The re-

TABLE II. Measured centroids and fine-structure splittings of pionic Ti and Fe 5-4 transitions.

		Measured centroid λ(mÅ) 5*g*-4*f*	Measured centroid λ(mÅ) 5*f*-4*d*	χ^2 per degree of freedom	Δλ(mÅ)	Δ*E*(eV)	
π-Ti	group I	306.395(10)	305.759(32)	0.7	0.636(34)	84.2(4.5)	mean 85.2(3.0)
	group II	306.331(34)	305.579(83)	0.9	0.752(91)	99.5(12.0)	
	group III	306.347(16)	305.711(28)	0.9	0.636(33)	84.2(4.3)	
π-Fe		219.032(9)	218.420(29)	1.0	0.612(30)		158.5(7.8)

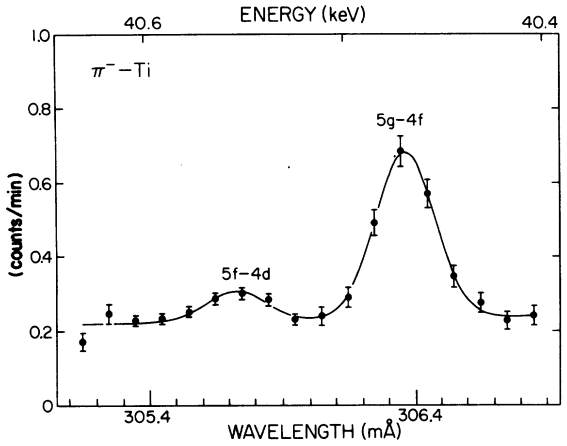

FIG. 2. Pionic Ti 5-4 transitions. (The ordinate has been scaled to read counts/min.)

sults of the centroids and the χ^2 per degree of freedom of the fit are given in Table II. The fitted curves are also shown in Figs. 2 and 3. The energy splitting $\Delta E = (E/\lambda)\Delta\lambda$ was obtained using a conversion factor E/λ based on calculated transition energies and the relation $E\lambda = 12\,398.52(3)$ eV Å.[12] The final results (weighted mean) are given in the last column of Table II.

The intensity ratios of the $5f$-$4d$ and $5g$-$4f$ transitions were found to be 0.19 ± 0.04 for Ti and 0.17 ± 0.05 for Fe. In comparison, the cascade program,[13] assuming statistical initial l distribution and no depletion in the L shell, furnishes values of 0.21 and 0.18, respectively, in agreement with the observations. A recent result by Delker *et al.*[3] studying the same Ti transitions yields $\Delta E = 87.6 \pm 1.8$ eV, and an intensity ratio of 0.164 ± 0.034, in good agreement with our work.

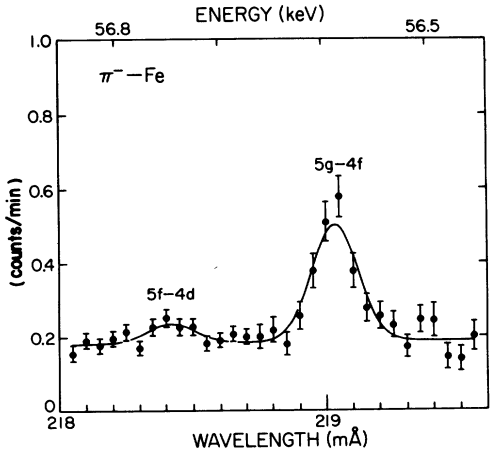

FIG. 3. Pionic Fe 5-4 transitions. (The ordinate has been scaled to read counts/min.)

SOLUTIONS OF THE KLEIN-GORDON EQUATION

In this section we discuss the various contributions to the binding energies for the $n = 4$ and 5 states in pionic Ti and Fe atoms. The principal contribution to the binding energy comes from the point Coulomb interaction. Smaller contributions arise from vacuum polarization, strong interaction, and electron screening. The numerical calculation of the energy levels is also discussed. The binding energy E is obtained by solving the Klein-Gordon equation.[14] For a point Coulomb field $V(r) = -Z\alpha/r$ the binding energy can be written as follows:

$$E = m(1 + (Z\alpha)^2/\{n - l - \tfrac{1}{2} + [(l+\tfrac{1}{2})^2 - (Z\alpha)^2]^{1/2}\}^2)^{-1/2}$$

$$\simeq m[1 - (Z\alpha)^2/2n^2 - (Z\alpha)^4/2n^4[n/(l+\tfrac{1}{2}) - \tfrac{3}{4}] + \cdots], \quad (1)$$

where m is the pion mass ($c = 1$).

It is interesting to note that the relativistic Schrödinger equation,[15]

$$[(p^2 + m^2)^{1/2} - Z\alpha/r]\psi = E\psi \quad (2)$$

gives the same bound-state energies up to terms $(Z\alpha/n)^4$ as the Klein-Gordon equation. The small differences arising in the comparison of terms $(Z\alpha/n)^6$ and higher will be discussed in the Appendix.

The electronic vacuum-polarization potential[16] of order $\alpha Z\alpha$ (Uehling potential) was added to the Coulomb potential using the method proposed by McKee.[17] The $\alpha^2 Z\alpha$ and $\alpha(Z\alpha)^3$ vacuum-polarization contribution were treated as perturbations using the tabulated values of Ref. 18. The finite nuclear size was folded into the Coulomb potential but the correction turned out to be negligibly small. The extended charge distribution was also folded into the vacuum-polarization correction.

The strong interaction effects in the transitions considered were small since the $5g$, $5f$, $4f$, and $4d$ orbits did not penetrate the nucleus appreciably. The corrections applied to the potential were obtained from the parametrization of Powers *et al.*,[19] which provides a good description for pionic-atom data for $6 \leq Z \leq 22$. When other standard sets of strong interaction parameters were employed, the resulting differences were less than 1 eV.

The electron screening potential of Vogel[18] was included and treated as a perturbation. It was assumed that inner electron shells of the pionic atoms were not ionized at the time when the x ray transitions under consideration were emitted. This assumption was recently carefully examined.[20]

Numerical solutions of the Klein-Gordon equation were obtained using the method described in Ref. 21. The size of the corrections to the eigen-

TABLE III. Calculated energies and fine-structure splittings of pionic Ti and Fe $5g$-$4f$ and $5f$-$4d$ transitions (in eV).

	Pionic Ti ($Z=22$, $A=48$)			Pionic Fe ($Z=26$, $A=56$)		
	$5g$-$4f$	$5f$-$4d$	Difference	$5g$-$4f$	$5f$-$4d$	Difference
Point Coulomb interaction	40 386.2	40 445.5	59.3	56 456.9	56 572.8	115.9
First-order vacuum polarization	82.5	108.5	26.0	137.1	173.9	36.8
High-order vacuum polarization	0.7	1.0	0.3	0.7	1.3	0.6
Strong interaction[a]	0.0	4.4	4.4	0.0	16.0	16.0
Electron screening[b]	−4.4	−5.9	−1.5	−5.3	−7.0	−1.7
Total energy	40 465.0	40 553.5	88.5	56 589.4	56 757.0	167.6
Wavelength (mÅ)	306.401	305.732	0.669	219.096	218.449	0.647

[a] The uncertainty is about 10%.
[b] We assume the presence of two $1s$ electrons.

value from vacuum polarization and strong interaction could easily be inspected by "turning off" the corresponding terms in the potential. The results of our calculation are shown in Table III. The point nucleus Coulomb term as well as all the corrections discussed above, are given for the $5g$-$4f$ and $5f$-$4d$ transitions in pionic Ti and Fe. The effect of nuclear motion beyond the reduced-mass correction pointed out by Seki[22] was calculated and found to be negligible; so were the effects of isotope shifts.

CONCLUSION

The angular-momentum dependence in bound states of pionic atoms as observed in the present experiment agrees to about 3–5% with the calculation based on relativistic equations for spin-zero particles. At this precision our experiment is able to confirm terms of order $(Z\alpha/n)^4$ in the expansion of the energy eigenvalues. The present precision is limited by the statistical accuracy attainable.

Higher pion stopping rates would open the possibility of exploring terms of order $(Z\alpha/n)^6$. As shown in the Appendix, the Darwin term gives a contribution of about 0.2 eV in the splitting of pionic Fe 5-4 transitions which is about 300 times smaller than the $(Z\alpha/n)^4$ terms. At this level of accuracy, however, uncertainties associated with the crystal spectrometer optics, as well as insufficient precision in present screening and strong-interaction calculations, may present a serious limitation.

APPENDIX

It is of interest to give physical interpretation to the various terms in the expansion of the bound-state eigenvalue [Eq. (1)]. At the same time one can compare the Klein-Gordon equation with the relativistic Schrödinger equation (2). This latter equation, also sometimes called "square-root Klein-Gordon equation" is not relativistically invariant when an external field is present.[23] The more satisfactory Klein-Gordon equation leads, however, to the well-known problems of negative energies and of "impossibility of a single-particle relativistic theory."[23] As far as the bound states are concerned, the differences between the two equations, although of fundamental importance, are numerically small.

In order to compare the two equations, one can use the Foldy-Wouthuysen transformation[24] and change the Klein-Gordon equation into a one component form. Performing the Foldy-Wouthuysen transformation twice, one obtains the Hamiltonian

$$H=m+\frac{p^2}{2m}-\frac{p^4}{8m^3}+\frac{p^6}{16m^5}-\frac{Z\alpha}{r}$$
$$-\frac{Z\alpha}{32m^4}[p^2,[p^2,1/r]]. \qquad \text{(A1)}$$

The second, third, and fourth terms in H are the expansion terms of the kinetic energy in powers of p/m. Identical terms are present in the relativistic Schrödinger equation. They describe the relativistic dependence of mass on velocity. The pion moves with different velocities in orbits with the same n but different l, and these relativistic effects will break the l degeneracy of the nonrelativistic Bohr formula. In particular, the $(Z\alpha/n)^4$ term in the expansion of the eigenvalue, Eq. (1), is obtained in the first-order perturbation treatment of the third term in Eq. (A1).

The last term in Eq. (A1) is present only in the Klein-Gordon equation. It is analogous to the Darwin term of the Dirac equation. Unlike the Darwin term, which contributes to the eigenvalue of order $(Z\alpha/n)^4$, the double commutator in Eq. (A1) con-

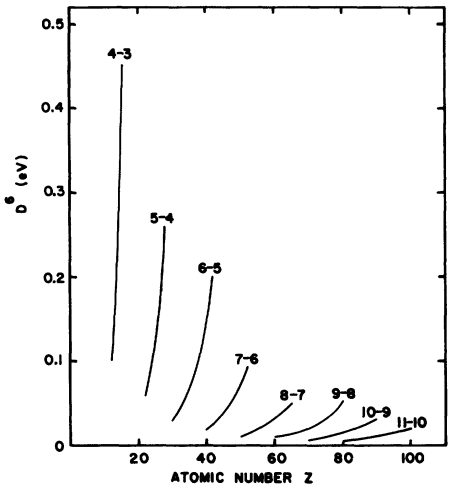

FIG. 4. Difference D^6 of energy splittings predicted by the Klein-Gordon equation and the relativistic Schrödinger equation, to order $(Z\alpha/n)^6$ for pionic transitions with energies between 20 and 40 keV.

tributes only in order $(Z\alpha/n)^6$. Evaluating it in first-order perturbation theory one obtains

$$\Delta_{nl} = -\frac{m}{16}\left(\frac{Z\alpha}{n}\right)^6 \frac{3n^3 - nl(l+1)}{(l+\frac{3}{2})(l+1)(l+\frac{1}{2})l(l-\frac{1}{2})}. \qquad \text{(A2)}$$

In order to distinguish between the eigenvalues of the Klein-Gordon and relativistic Schrödinger equation, one would have to observe the effect of the term (A2) on the x-ray energy splitting. The size of such a difference in the splitting, for x rays of 40–60 keV, is shown in Fig. 4. Its observation must await improvements in experimental accuracy and in the accuracy of calculating various theoretical correction factors.

ACKNOWLEDGMENTS

We wish to thank Dr. Louis Rosen and his staff at LAMPF for their hospitality and cooperation. Professor Valentin Telegdi and Dr. Michael Nieto helped us with their clarifying comments on the relativistic equations. We would also like to thank Professor Paul Lee for enlightening discussions and Mr. Mark Manley for valuable assistance during the experiment. One of us (K.-C. Wang) has received partial support from the National Science Foundation under Grant No. PHY75-23206. E. Bovet wishes to acknowledge support from the Swiss National Science Foundation. This work was supported by the Department of Energy under Grants Nos. DE-AC-03-76-ER00063 and AT[11-1]-2197.

*Present address: Physics Department, University of California, Irvine, California 92717.
†Present address: Boston University, Boston, Massachusetts 02215.

[1]A. L. Carter, M. S. Dixit, M. K. Sundaresan, J. S. Wadden, P. J. S, Watson, C. K. Hargrove, E. P. Hincks, R. J. McKee, H. Mes, H. L. Anderson, and A. Zehnder, Phys. Rev. Lett. 37, 1380 (1976).
[2]K.-C. Wang, F. Boehm, A. A. Hahn, H. E. Henrikson, J. P. Miller, R. J. Powers, P. Vogel, J.-L. Vuilleumier, and A. R. Kunselman, Phys. Lett. 79B, 170 (1978).
[3]L. Delker, G. Dugan, C. S. Wu, D. C. Lu, A. J. Caffrey, Y. T. Cheng, and Y. K. Lee, Phys. Rev. Lett. 42, 89 (1979).
[4]K.-C. Wang, Ph.D. thesis, California Institute of Technology, 1979 (unpublished).
[5]H. E. Henrikson and F. Boehm, Nucl. Instrum. Methods 121, 269 (1974).
[6]Manufactured by the Space Technology Products Laboratory of the General Electric Company, King of Prussia Park, Pennsylvania.
[7]O. I. Sumbaev, Zh. Eksp. Teor. Fiz. 54, 1352 (1968) [Sov. Phys.—JETP 27, 724 (1968)].
[8]E. J. Seppi, H. Henrikson, F. Boehm, and J. W. M. DuMond, Nucl. Instrum. Methods 16, 17 (1962).
[9]J. A. Bearden, Rev. Mod. Phys. 39, 78 (1967); E. R. Cohen, At. Data Nucl. Data Tables 18, 587 (1976).
[10]P. L. Lee, Nucl. Instrum. Methods 144, 363 (1977).
[11]K.-C. Wang, A. A. Hahn, and F. Boehm, Phys. Rev. A 17, 1735 (1978).
[12]E. R. Cohen and B. N. Taylor, J. Phys. Chem. Ref. Data 2, 663 (1973).
[13]V. R. Akylas and P. Vogel, Comp. Phys. Commun. 15, 291 (1978).
[14]A. S. Davydov, *Quantum Mechanics* (Pergamon, Oxford, 1965), 1st ed., pp. 208ff.
[15]M. L. Goldberger and K. M. Watson, *Collision Theory* (Wiley, New York, 1964), p. 24.
[16]R. C. Barrett, S. J. Brodsky, G. W. Erickson, and M. H. Goldhaber, Phys. Rev. 166, 1589 (1968).
[17]R. J. McKee, Phys. Rev. 180, 1139 (1969).
[18]P. Vogel, At. Data Nucl. Data Tables 14, 599 (1974).
[19]R. J. Powers, K.-C. Wang, M. H. Hoehn, E. B. Shera, H. D. Wolfahrt, and A. R. Kunselman, Nucl. Phys. A 336, 475 (1980).
[20]E. Bovet, F. Boehm, R. J. Powers, P. Vogel, K.-C. Wang, and A. R. Kunselman, Phys. Lett. 92B, 87 (1980).
[21]D. K. Anderson, D. A. Jenkins, and R. J. Powers, Phys. Rev. 188, 9 (1969); Phys. Rev. Lett. 24, 71 (1970).
[22]R. Seki, Phys. Lett. 58B, 49 (1975).
[23]J. Sucher, J. Math. Phys. 4, 17 (1963).
[24]J. D. Bjorken and S. D. Drell, *Relativistic Quantum Mechanics* (McGraw-Hill, New York, 1964), pp. 202ff.